Preparation and self assembly of Fe-Au Core-Shell Magnetic Nanoparticles into Three-Dimensional Crystal for Nanomagnetic Applications

Wan-Chi Chen,[†] Kung-Hwa Wei,[*,†] Jung Y. Huang,[‡] Jeng-Yi Tsai,[§] and Jiunn-Yuan Lin,[§] U-Ser Jeng,[#] and Jin-Ming Chen[#]

[†] *Department of Materials Science and Engineering,* [‡] *Department of Photonic,* [§] *Institute of Physics, Chiao Tung University, Taiwan 1001 Ta Hsueh Road , Hsinchu 30050 , Taiwan ,and* [#] *National Synchrotron Radiation Research Center , 101 Hsin-Ann Road , Science-Based Industrial Park , Hsinchu, 30077, Taiwan*

Magnetic nanoparticles (NPs) have generated a great deal of interest because of their unique magnetic properties, which make them very appealing structures from both theoretical and technological points of view. Below a critical size, magnetic particles become single domain and exhibit unique phenomena such as superparamagnetism,[1a] quantum tunneling of the magnetization,[1b] and unusual large coercivities.[1c] The fabrication of these NPs, which can be effected in a number of ways,[2] has inspired a wide range of applications within the fields of medical diagnosis, drug delivery, cell separation, and information storage.[3] The greatest challenges in the synthesis of iron (Fe) NPs are controlling the particle size and the degree of monodispersity and preventing oxidation. A non-magnetic shell, such as one prepared from gold (Au), surrounding a Fe nanoparticle potentially could serve as a protection layer,[4] provide an enhanced optical response through surface plasmon excitation, and present an accessible surface for further functionalization. Three-dimensional (3D) crystals self-assembled from these Fe-Au core-shell NPs (Fe-Au NPs) would not only be interesting model systems for nano-magnetic materials but also could offer great potential for use in single-electron transistors and spin-dependent applications.[5]

In this communication, we report the successful synthesis of near-monodisperse Fe-Au NPs and their self-assembly into a robust 3D crystalline structure. In addition, we provide evidence from X-ray absorption spectroscopy (XAS) that verifies that the core of each nanoparticle in the self-assembled crystal is pure Fe. We synthesized the Fe–Au NPs using water-in-oil microemulsions in which the dispersity in the sizes of these NPs can be controlled by adjusting the water content.[6] We note that an approach toward the self-assembly of Au NPs into a robust 3D nanocrystal was reported recently.[7] Scheme 1 depicts the schematic processes we used to synthesize the Fe – Au NPs (steps A–B) and the self-assembly of the 3D Fe – Au crystal (steps C–E). In brief, first we synthesized the Fe – Au NPs in a reverse micelle system comprising a surfactant (cetyltrimetylammonium bromide, CTAB), water (aqueous $FeSO_4$ and $HAuCl_4$ solutions), and an oil (octane), as reported in the literature.[4] We then used 1-dodecanethiol in step B to modify the surfaces of the Fe – Au NPs. Finally, we added CTAB and tetraethylorthosilicate (TEOS) to form a self-assembled Fe – Au artificial crystal.[6b,7]

Fig. 1a presents a TEM image of the resulting Fe – Au NPs. The inset to Fig. 1a displays the lattice image of a nanoparticle. The core of the nanoparticle appears slightly darker than the shell because of the difference between the electron penetration efficiencies in Fe and Au. The average size of the Fe – Au NPs was ca. 5.5 nm, i.e., a 4-nm-diameter Fe core surrounded by a 0.75-nm-thick Au shell. This core-shell structure has been confirmed by an inductively coupled plasma-mass spectrometer.[6b] A small-angle X-ray scattering pattern of the Fe – Au NPs artificial crystal with synchrotron radiation indicated that it is a face-centered cubic structure. (See supporting information)[6b]

Scheme 1. The synthetic strategy for preparing the Fe – Au NPs and the Fe – Au artificial crystal.

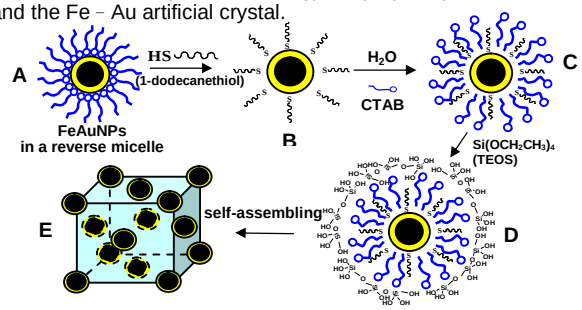

One of the challenges in synthesizing Fe NPs is preventing the Fe from oxidization. We note that direct evidence for the existence of pure Fe NPs through any synthetic scheme has yet to be reported.[2b,4] For example, even when Au shells were used to passivate Fe cores, the Fe atom was still readily oxidized during the synthetic process.[8] In this study, we used the Fe atom's *L*-edge to characterize the chemical state of the Fe cores in both the Fe – Au NPs and the self-assembled Fe – Au crystals. Fig. 1b presents the *L*-edge spectra of Fe in these samples and in three reference materials: Fe_2O_3, Fe_3O_4, and Fe powder. All the reference spectra we obtained are consistent with those reported in the literature.[9] The L_3 spectrum of the Fe – Au NPs exhibits two peaks at 708 and 710 eV that can be attributed to Fe oxides, but the ratio of these spectral peaks' intensities (708 to 710 eV) is larger than those observed for the Fe oxides, which suggests that our Fe – Au NPs were oxidized only partially. Most noticeably, the spectrum of the artificial crystal of self-assembled Fe – Au NPs exhibits only a single peak at 708 eV, which indicates that the core of the nanoparticle comprises pure Fe. We believe that this spectrum provides the first direct evidence for the synthesis of pure Fe NPs, albeit those containing a Au shell and confined within a silica matrix. The mechanism through which the Fe oxides within the Fe – Au NPs are transformed into pure Fe cores within the artificial crystal remains unclear at this moment. There are some reports in the literature,[10] however, that describe how Au on a Fe_2O_3 metal oxide can effect catalytic functions toward several reactions, including hydrogenation, reduction, and oxidation. In the presence of light, sulfur (S) atoms can desorb from the surface of metal oxide-supported Au NPs (S-Au/Fe_2O_3) in water at room temperature. Furthermore when silanes are attached to Au surfaces, hydrogen atoms can be released to form Au–Si covalent bonds. Therefore, we suspect that the system displayed in Scheme 1 might occur—a reduction of iron oxide-Au

NPs in the presence of TEOS—to convert the S-Au/Fe oxide NPs into S-Au/Fe NPs.

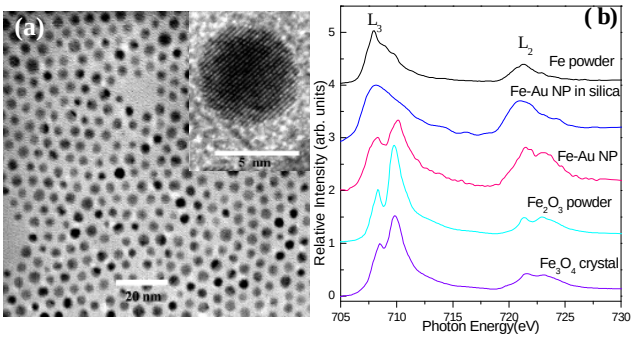

Figure 1 (a) TEM image displaying the dispersed Fe-Au NPs. The inset presents an enlarged image of one nanoparticle to indicate the lattice image of the shell. (b) The L-edge XAS spectrum of Fe in Fe powder, Fe_3O_4, Fe_2O_3, Fe – Au NPs, and the Fe – Au artificial crystal.

Fig. 2 displays the magnetization properties of Fe oxide–Au NPs and the Fe–Au artificial crystal within the silica matrix at different temperatures. Obtain these results required measuring and subtracting the diamagnetic contributions of the surfactant layer and the silica. The Fe oxide–Au NPs are superparamagnetic at 300 and 50 K, and we observed only a very small coercive field (H_c < 10 Oe, not visible on this scale) at 2 K. The Fe – Au artificial crystal exhibits a clear coercive field (H_c = 70 Oe) at 2 K. The hysteresis of the Fe – Au artificial crystal is not the typical curve observed for ferromagnetism, which suggests that a marginal transit from superparamagnetism to ferromagnetism occurs at this temperature. Thermal fluctuations prevent the spontaneous magnetization of NPs from pointing in a fixed direction when the particles are smaller than the critical size, as suggested by Neel.[11] For a particle having uniaxial anisotropy, $\Delta E = KV$ (at H = 0), the condition for superparamagnetism could be expressed as $KV = 25\ kT_B$, where V is the volume of the nanoparticle, K is the anisotropy energy, k is the Boltzmann constant, and T_B is the blocking temperature. Therefore, T_B is proportional to d^3, where d is the diameter of the nanoparticle. For d = 7 nm, it has been reported that Fe–Fe_3O_4 NPs had a value of T_B of 35 K.[2b] Although their composition is different, we can estimate that Fe cores having d = 4 nm would have a value of T_B of 6 K. We observe a hysteresis loop at 2 K for the artificial crystal sample, which does not contradict this estimate. The clear existence of H_c at 2 K for the Fe – Au artificial crystal is in sharp contrast to that observed for the Fe – Au NPs. This contrast may be due to the different degrees of oxidation of the Fe cores in the two materials, which would provide additional indirect evidence for their different chemical states. Another possibility is that the ordered Fe – Au artificial crystal may lead to an additional anisotropy energy, which certainly would enhance ferromagnetism, relative to that of random NPs. Because both Fe oxide–Au NPs and the Fe – Au artificial crystal are superparamagnetic at 50 K, we can fit the measured data in Fig. 2 to the Langevin paramagnetic function: $M(x) = \coth(x) - 1/x$, with $x = \mu H/kT$. The line of best fit (see the solid curve) yields $\mu = 210\mu_B$ for the Fe oxide–Au NPs and $400\mu_B$ for the Fe – Au artificial crystal. By assuming that the core of each Fe oxide–Au NPs has a α-Fe_2O_3 crystal structure, we estimate that at 50 K and a magnetic flux density of 1 T, each Fe^{3+} ion in the NPs has a magnetic moment of 0.23 μ_B. We also calculate that each Fe atom in single Fe – Au nanocrystal has a magnetic moment of 0.44 μ_B. The value for the Fe–Au artificial crystal is about five times smaller than that observed in bulk Fe. This can be explained partly by the fact that magnetic NPs appear to have a reduction of the saturation magnetization[12] due to competing antiferromagnetic exchange interactions at the surface, which causes random canting of the particles' surface spins.[13] This phenomenon has also been argued in favor of a surface origin[12,14] and a finite size effect,[12,15] but no clear conclusions regarding the origin of the effect have been provided.

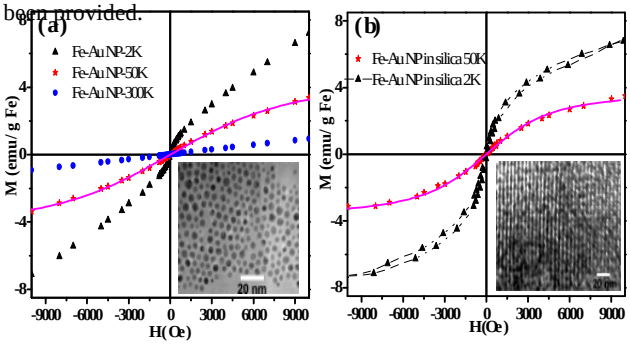

Figure 2. Plots of magnetization (M) vs. magnetic field (H) of the (a) Fe – Au NPs at 300, 50, and 2 K and (b) the self-assembled Fe – Au ordered structure at 50 and 2 K. The solid curves represent best fits of the data to the Langevin paramagnetic model.

Acknowledgement. We acknowledge the National Science Council for funding this work through grants NSC92-2120-M-009-009 and NSC93-2112-M-009-015.

Supporting Information Available: Experimental details, Fe – Au artificial crystal structural characterization, and TEM images. This material is available free of charge via the Internet at http://pubs.acs.org.

References

1.(a) Kittel, C. *Phys. Rev.* **70**, 965 (1946). (b) Chudnovsky E. M. and Gunther, L. *Phys. Rev. Lett.* **60**, 661 (1988). (c) Kneller, E. F. and Luborsky, F. E. *J. Appl. Phys.* **34**, 656 (1963).
2.(a) Suslick, K. S. Fang, M. and Hyeon, T. *J. Am. Chem. Soc.* **118**, 11960 (1996). (b) Farrell, D. Majetich, S. A. and Wilcoxon, J. P. *J. Phys. Chem. B* **107**, 11022 (2003). (c) Park, J. An, K. Hwang, Y. Park, J.-G. Noh, H.-J. Kim, J.-Y. Park, J.-H. Hwang, N.-M. and Hyeon, T. *Nature materials* **3**, 891 (2004). (d) Sun, S. Zeng, H. Robinson, D. B. Raoux, S. Rice, P. M. Wang, S. X. and Li, G. *J. Am. Chem. Soc.* **126**, 273 (2004).
3.(a) Chung, S. H. Hoffmann, A. Bader, S. D. Liu, C. Kay, B. Makowski, L. and Chen, L. *Appl. Phys. Lett.* **85**, 2971 (2004). (b) Tartaj, P. Morales, M. P. Veintemillas-Verdaguer S. Goonzález-Carreño T. and Serna, C. J. *J. Phys. D: Appl. Phys.* **36**, R182 (2003). (c) Li, J. Mirzamaani, M. Bian, X. Doerner, M. Duan, S. Tang, K. Toney, M. Arnoldussen, T. and Madison, M. *J. Appl. Phys.* **85**, 4286 (1999).
4.(a) Zhou, W. L. Carpenter, E. E. Lin, J. Kumbhar, A. Sims, J. and O'Connor, C. J. *Eur. Phys. J. D.* **16**, 289 (2001). (b) Cho, S.-J. Kauzlarich, S. M. Olamit, J. Liu, K. Grandjean, F. Rebbouh, L. Lang, G. J. *J. Appl. Phys.* **95**, 6804 (2004).
5.(a) Davidovic, D. and Tinkham, M. *Appl. Phys. Lett.* **73**, 3959 (1998). (b) Black, C. T. Murray, C. B. Sandstrom, R. L. and Sun, S. *Science* **290**, 1131 (2000)
6. (a) Pileni, M. P. *Langmuir* **13**, 3266 (1997). (b) See supporting information.
7. Fan, H. Yang, K. Boye, D. M. Sigmon, T. Malloy, K. J. Xu, H. López, G. P. and Brinker, C. J. *Science* **304**, 567 (2004)
8. Ravel, B. Carpenter, E. E. and Harris, V. G. *J. Appl. Phys.* **91,** 8195 (2002)
9. Regan, T. J. Ohldag, H. Stamm, C. Nolting, F. Lüning, J. Stöhr, J. and White, R. L. *Phys. Rev. B* **64**, 214422 (2001)
10. (a) Finch, R. M. Hodge, N. A. Hutchings, G. J. Quentin, A. M. Siddiqui, M. R. H. Wagner, F. E. and Whyman, R. *Phys. Chem. Chem. Phys.* **1**, 485 (1999). (b) Tada, H. Soejima, T. Ito, S. and Kobayashi, H. *J. Am. Chem. Soc.* **126**, 15952 (2004). (c) Owens, T. M. Nicholson, K. T. Holl, M. M. B. and Süzer, S. *J. Am. Chem. Soc.* **124**, 6800 (2002).
11. Néel, L, *C. R. Acad. Sci.* **228**, 664 (1949)
12. Martínez, B. Obradors, X. Balcells, Ll. Rouanet, A. and Monty, C. *Phys. Rev. Lett.* **80**, 181 (1998)
13. Coey, J. M. D. *Phys. Rev. Lett.* **27**, 1140 (1971).
14. Morrish, A. Hanada, H. K. and Schurer, P. J. *J. Phys. C* **37**, 6 (1976).
15. Parker, F. T. Foster, M. W. Margulies, D. T. and Berkowitz, A. E. *Phys. Rev. B* **47**, 7885 (1993)

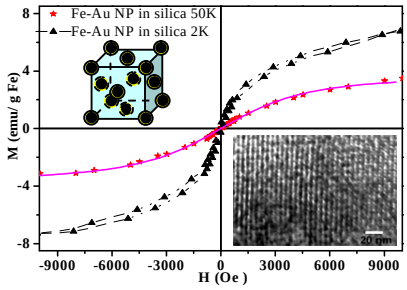

Near-monodisperse Fe – Au NPs have been synthesized successfully and self-assembled into a robust three-dimensional (3D) crystalline structure. X-Ray near-edge absorption spectroscopy verifies that the cores in the 3D artificial crystal comprise pure iron. This approach allows the preparation of nanoparticles in their pure metal state without oxidization. Each Fe atom in the Fe – Au artificial crystal possesses a magnetic moment of 0.44 μB.